Power Frequency Control of the Grid using PMSG-Based Wind Farm Connected by HVDC Link Controlled by a New Method Based on Fuzzy Logic Controller

Ali Mastanabadi, Gholamreza Aghajani*, Davar Mirabbasi

Department of Electrical Engineering, Ardabil branch, Islamic Azad University, Ardabil, Iran, aghajani_gholamreza@yahoo.com

Abstract

By development of the power system in presence of the sustainable energies, the issue of grid frequency control is becoming more important. In traditional power systems, the frequency is mostly controlled by the hydroelectric power plants. This makes it troublesome in cases of dry spell or the absence of the hydro power plants. In this paper, a new method based on using wind farm equipped with PMSG, connected through HVDC link and controlled by fuzzy logic controller, is proposed to investigate the feasibility of using wind farms to improve the frequency control performance. The proposed system is tested on a four-area grid and simulated in MATLAB /Simulink. It is concluded that the best performance, which is up to 26% improvement in settling time of the frequency deviation, is achieved by the proposed system in comparison to using the traditional control method and using wind farm controlled by conventional controllers.

Keywords: DFIG (Doubly Fed Induction Generator), Load Frequency Control (LFC), Voltage Source Converter (VSC), Permanent Magnet Synchronous Generator (PMSG), Wind Energy Conversion Systems (WECS).
Article history: Submitted 2022-12-06; Revised 2022-12-01; Accepted 2022-12-16. Article Type: Research paper

https://doi.org/10.30495/ijsee.2022.1974382.1241

1. Introduction

In the power grid containing Wind Energy Conversion Systems (WECS) and conventional synchronous generators, frequency stability is a key index which is commonly supported by the synchronous generators. Due to the large installation of WECSs with a high penetration, limited synchronous generators could not be able to provide the required active power for frequency regulation. Stochastic nature of wind energy makes power balance difficult. Meanwhile, load change may lead to frequency instability [1]. The limitation on the regulating ability of the synchronous generator brings a serious challenge to frequency stability of an isolated grid. Consequently, there is an urgent need for WECSs to participate in regulating frequency [1]. Therefore, the power grid frequency control is a very vital issue. In traditional power systems, the frequency of the grid is usually controlled by the hydro power plants, which are usually gained by rapid dynamic response. According to the mentioned issues, it can be realized that in case of expansion of the power system, increasing the capacity of hydropower plants is inevitable. This requires large investment and is not possible in regions facing drought or water scarcity. On the other hand, due to the increasing use of renewable energies, especially wind farms, a large capacity of power generation is available. This is very attractive, but the challenge ahead is the variability and unpredictability of the wind speed as the input power of wind farms, which makes its power production dependent on the wind speed. Therefore, by controlling the output power of wind turbines in a rapid dynamic, it can be well-involved in controlling the frequency of the power system. As wind farms are generally not considered in frequency regulation due to their technical limitations, therefore, there is a need to design a control system for the participation of wind farms in controlling the frequency of the grid. In the following, it is assumed to review the relevant research in this field and investigate their advantages and disadvantages. The contribution of WECS in power frequency control is mainly categorized in three methods. Some are based on energy storage systems, some of them are based on pitch angle

control and some other power electronics equipment. In various researches, several methods were used to control the frequency of the power grid in the presence of wind turbines. As an example, in [2]-[5], researchers evaluated the involvement of wind farms in frequency support by several energy storage systems controlled automatically. There are several similar works such as [6]-[10] used battery and super capacitor to control wind farm active power. In [6] researchers proposed a method based on a super capacitor and a DC/DC converter to control the output power of a wind turbine. In [7], an attractive method based on using hybrid energy storage systems was proposed. The researchers used the super capacitor and kinetic energy, stored in the turbine shaft to control the wind turbine power. Authors in [8] suggested using a battery/wind hybrid system to overcome unpredictability of the wind farms generated power. Other similar research presented a method based on a PV/Wind/Battery hybrid system considering demand response [9]. In [10], authors proposed a method based on another hybrid system. They proposed a new control system for a wind/super capacitor/ battery to manage wind turbine power generation in frequency control. Although in [10] the control system is so attractive, but it is not appropriate enough to control the frequency of the large scale systems. Authors in [11]-[16] used DFIG- based wind turbine with different configuration to coordinate in power frequency control of the grid. Although these system methods may be cheaper than the methods used in the previous studies, but may not perform well in severe wind changes. This is because in DFIG generators, a maximum amount of %30 of the generator output power can be controlled by the electronic power control unit. In [17], researchers used a wind farm to control the frequency of a local system using a pitch angle control method. Although it gains from relative simplicity in implementation, but it is not rapid enough to overcome the instantaneous demand power fluctuations. Moreover, it has high depreciation, may not be responsive in the power grid. Researchers in [18]-[22] used the rotor inertia to control the frequency of the grid. However, using rotor inertia or flywheel systems is appropriate for small systems. Authors in [23] investigated several aspects of this method to control the power of wind turbine systems through pitch angle system. In [23] a case study based on DFIG base wind turbine connected to the grid was investigated to contribute the frequency of the grid. The proposed main technique was based on pitch angle and speed rate control system of the turbines. Although the results were satisfying but the case was not studied in a multi-connected area. Some other studies, such as [24]-[27] used the PMSG based wind turbines connected to the grid controlled by fuzzy logic controller. It is illustrated that the system equipped with wind turbines has performed better in frequency control of the grid rather than in the absence of wind turbines. But the issue that was not considered was the power grid is assumed as an infinite bus, and the effect of the presence of different areas and inter-area transmission lines were not considered. The other important point is that the wind speed fluctuation in the simulation process is not considered, and it is assumed constant. Therefore, the capability of the proposed system in producing the desired active power in the presence of wind speed variations is not clear. Another method based on frequency regulation at a wind farm using time-varying inertia and droop controls was investigated in [28]. Authors in [29] presented a distributed synchronized control system in grid integrated wind farms to improve the primary frequency regulation. In [30] researchers proposed a control method for offshore wind turbines connected to diode-rectifier-based HVDC Systems to mitigate the frequency deviation of the grid. Moreover, in [31], a new control scheme for fast frequency support from HVDC connected offshore wind farm in a low inertia system is presented. The proposed system is generally appropriate for low inertia systems. A control method based on Two-Level combined control scheme of VSC-MTDC is proposed in [32] cooperating wind farm in frequency control of the grid. A solution based on double-layer feedback control method for synchronized frequency regulation of PMSG-based wind turbines is investigated in [33]. Some other similar articles such as [34] proposed an optimal fuzzy logic-based controller equipped with DFIG wind turbine to control the frequency in an off-grid power system. The proposed method has a better performance in frequency control of the grid rather than other conventional methods and finally, in [35], the authors overviewed the frequency-control technologies for wind farms and summarized them. Fig.1 illustrates a brief analysis and synthesis studies of power frequency control.

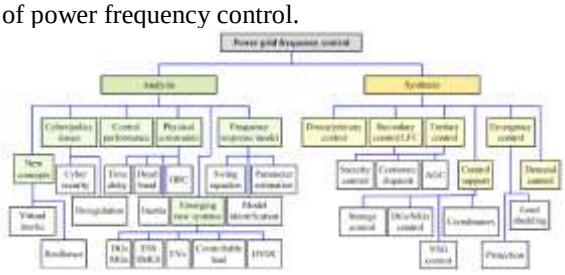

Fig. 1. Analysis and synthesis studies of power frequency control [36].

2. Modeling of PMSG-based Wind Turbine

The wind energy conversion system (WECS) used in this article includes a wind turbine,

PMSG, back to back HVDC-light link, its VSC converter and transformer. In this system, wind energy is extracted by wind turbines and transmitted to a three-phase PMSG through a constant speed ratio gearbox. The gearbox converts mechanical energy into electrical energy and, finally, transmits it through a HVDC link connected to the grid.

A) Wind Turbine Modeling

The wind turbine extracted power, ($P_{Extracted}$) and the mechanical torque (T_m) are as the following equations [37].

$$P_{Extracted} = \frac{1}{2} C_p(\lambda,\beta)\rho A V_w^{\ 3} \quad (1)$$

$$\lambda = \frac{R\omega}{V_w} \quad (2)$$

$$T_m = \frac{P_{Extracted}}{\omega} \quad (3)$$

where, $C_p(\lambda,\beta)$ is the efficiency of the wind turbine, which is dependent on the tip speed ratio (λ) and the pitch angle (β) of the turbine blades. In the above equations, ρ is the air density and is equal to $1.28 kg/m^3$, ω is the rotational speed of the turbine in rad/s, A is the wind turbine blades sweeping area in m^3 and finally V_w is the wind speed in m/s. Although the pitch angle control system is a common system for controlling the power of wind turbines, it can usually not be used to control the wind turbine during a fault condition due to its slow dynamic operation. Fig. 1 shows the $C_p(\lambda,\beta)$ curve, given by Eq. (4), for different pitch angels [37].

$$C_P(\lambda,\beta) = C_1\left(C_2 \frac{1}{\Lambda} - C_3\beta - C_4\beta^{C_5} - C_6\right)e^{-\frac{C_7}{\Lambda}} \quad (4)$$

Where Λ is given by Eq. (5). The coefficients $c_1 - c_9$ are different for various wind turbines and are selected as listed in Table 1 [37].

$$\frac{1}{\Lambda} = \frac{1}{\lambda + C_8\beta} - \frac{C_9}{1+\beta^3} \quad (5)$$

A) PMSG Modeling in d-q frame

The permanent magnet synchronous generator (PMSG) is one of the conventional generators used in wind turbine systems. The modeling of this type of generator in d-q frame is proposed in the following. Using the Fig. 3, the direct and quadrature voltage of the stator can be written as Eq. (6) [37].

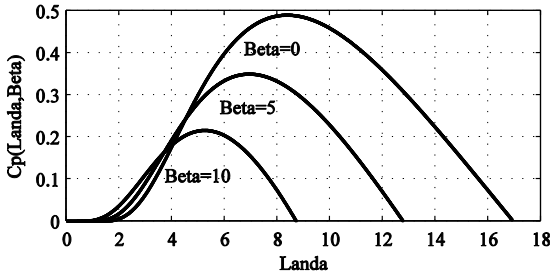

Fig. 2. $C_p(\lambda,\beta)$ curve [37]

Table.1.
Wind turbine coefficients and parameters [37]

C_1	C_2	C_3	C_4	C_5	C_6	C_7	C_8	C_9
0.44	125	0.4	0.02	2	6.94	16.5	0.08	0.0035

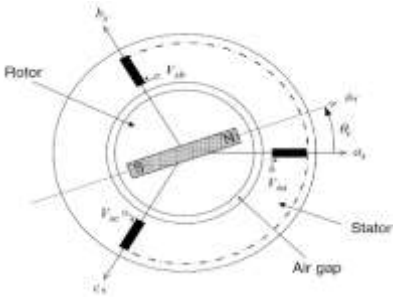

Fig. 3. PMSG schematic [37]

$$\begin{bmatrix} v_d \\ v_q \end{bmatrix} = \begin{bmatrix} L_d & 0 \\ 0 & L_q \end{bmatrix} \begin{bmatrix} \frac{di_d}{dt} \\ \frac{di_q}{dt} \end{bmatrix} + \begin{bmatrix} R_s & 0 \\ 0 & R_s \end{bmatrix} \begin{bmatrix} i_d \\ i_q \end{bmatrix} + \begin{bmatrix} -L_q p\omega_r i_q \\ L_d p\omega_r i_d + \lambda p\omega_r \end{bmatrix} \quad (6)$$

Where L_d, L_q, v_d, v_q, i_d, i_q and R_s are the stator's direct and quadrature axis inductances, voltages and currents and resistance, respectively. Also p is the Laplace differential operator, ω_r is the rotational speed of the rotor and λ is the flux linkage of the machine. In PMSGs which are not salient pole machines, the direct and quadrature axis inductances of the machine are as the same, thus $L_d = L_q = L_s$. By applying the Krichhoff's law on the stator's winding Eq. (7) can be written as below.

$$\frac{d\lambda_s}{dt} = v_s - R_s i_s \quad (7)$$

By converting the machine's parameters from the three-phase frame into the d-q frame, the Eq. (7) can be modified as Eq. (8) and Eq. (9).

$$\frac{d(\vec{\lambda}_{dq}\, e^{j\omega_s t})}{dt} = \vec{V}_{dq} - R_s \vec{i}_{dq}\, e^{j\omega_s t} \quad (8)$$

$$\frac{d}{dt}\begin{bmatrix}\lambda_d\\ \lambda_q\end{bmatrix}=\begin{bmatrix}0 & \omega_s\\ -\omega_s & 0\end{bmatrix}\begin{bmatrix}\lambda_d\\ \lambda_q\end{bmatrix}+\begin{bmatrix}-R_s & 0\\ 0 & -R_s\end{bmatrix}\begin{bmatrix}i_d\\ i_q\end{bmatrix}+\begin{bmatrix}v_{sd}\\ v_{sq}\end{bmatrix} \quad (9)$$

Where v_{s_d} and v_{sq} are the stator's direct and quadrature axis voltages. Also, the electrical active power absorbed by the machine can be determined as the following equations. Where the λ_d, λ_q and ω_s are the direct and quadrature axis flux linkage and the synchronous rotational speed.

$$P=\frac{3}{2}\begin{bmatrix}i_d\\ i_q\end{bmatrix}^T\begin{bmatrix}v_{sd}\\ v_{sq}\end{bmatrix}=\frac{3}{2}\begin{bmatrix}i_d\\ i_q\end{bmatrix}^T\left\{\frac{d}{dt}\begin{bmatrix}\lambda_d\\ \lambda_q\end{bmatrix}-\begin{bmatrix}0 & \omega_s\\ -\omega_s & 0\end{bmatrix}\begin{bmatrix}\lambda_d\\ \lambda_q\end{bmatrix}+\begin{bmatrix}-R_s & 0\\ 0 & -R_s\end{bmatrix}\begin{bmatrix}i_d\\ i_q\end{bmatrix}\right\} \quad (10)$$

$$P=\frac{3}{2}R_s(i_d{}^2+i_q{}^2)+\frac{3}{2}(i_d\frac{d\lambda_d}{dt}+i_q\frac{d\lambda_q}{dt})+\frac{3}{2}\omega_s(\lambda_d i_q-\lambda_q i_d) \quad (11)$$

The electromagnetic torque can be deduced from Eq. (11).

$$T_e=\frac{P}{\omega_r}=\frac{3}{2}p(\lambda_d i_d-\lambda_q i_d) \quad (12)$$

$$T_e=\frac{3}{2}p[\lambda_m i_q+(L_d-L_q)i_d i_q) \quad (13)$$

$$T_e=\frac{3}{2}p\lambda i_q \quad (14)$$

$$i_{q_{ref}}=-\frac{T_{Turbine}}{\frac{3}{2}p\lambda} \quad (15)$$

2.3. VSC Average Model

In this section, the modeling of the VSC is presented. It is connected to the PMSG to control the torque, output power and the rotational speed. Fig. 4 illustrates the simplified circuit of this system [37].

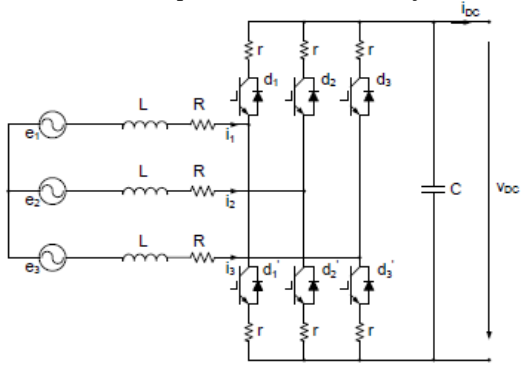

Fig. 4. Model of the VSC [36].

In Fig. 3, by applying the Kirchhoff's law, the Eq. (16) can be inferred as follows.

$$L\frac{di_a}{dt}+Ri_a=V_{ta}-U_a \quad (16)$$

$$L\frac{di_b}{dt}+Ri_b=V_{tb}-U_b$$

$$L\frac{di_c}{dt}+Ri_c=V_{tc}-U_c$$

Where, V_{ta}, V_{tb}, V_{tc} are the output voltages of the VSC. By using Fourier's series of these periodical voltages, the Eq. (16) can be rewritten as follows [37].

$$\begin{aligned}
L\frac{di_a}{dt}+Ri_a&=(-U_a+\frac{1}{T_s}\int_{t-T_s}^{T_s}V_{ta}(\tau)d\tau)+\sum_{h=1}^{\infty}[a_{a_h}\cos(h\omega_s\tau)+b_{a_h}\sin(h\omega_s\tau)]\\
L\frac{di_b}{dt}+Ri_b&=(-U_b+\frac{1}{T_s}\int_{t-T_s}^{T_s}V_{tb}(\tau)d\tau)+\sum_{h=1}^{\infty}[a_{b_h}\cos(h\omega_s\tau)+b_{b_h}\sin(h\omega_s\tau)]\\
L\frac{di_c}{dt}+Ri_c&=(-U_c+\frac{1}{T_s}\int_{t-T_s}^{T_s}V_{tc}(\tau)d\tau)+\sum_{h=1}^{\infty}[a_{c_h}\cos(h\omega_s\tau)+b_{c_h}\sin(h\omega_s\tau)]
\end{aligned} \quad (17)$$

$$a_{i_h}=\frac{2}{T_s}\int_{t-T_s}^{T_s}(V_{ti}(\tau)\cos(h\omega_s\tau)d\tau$$

$$b_{i_h}=\frac{2}{T_s}\int_{t-T_s}^{T_s}(V_{ti}(\tau)\sin(h\omega_s\tau)d\tau$$

Eq. (17) is a set of differential equations which has AC and DC responses. However, by using the superposition law, these two components can be separately analysed. The AC component is negligible if the switching frequency is too larger than the R/L value. Therefore, the Eq. (17) can be rewritten as follows.

$$\begin{aligned}
L\frac{di_a}{dt}+Ri_a&=(-U_a+\frac{1}{T_s}\int_{t-T_s}^{T_s}V_{ta}(\tau)d\tau))\\
L\frac{di_b}{dt}+Ri_b&=(-U_b+\frac{1}{T_s}\int_{t-T_s}^{T_s}V_{tb}(\tau)d\tau))\\
L\frac{di_c}{dt}+Ri_c&=(-U_c+\frac{1}{T_s}\int_{t-T_s}^{T_s}V_{tc}(\tau)d\tau))
\end{aligned} \quad (18)$$

For a sinusoidal PWM, Eq. (19) can be rewritten as following.

$$\begin{aligned}
L\frac{di_a}{dt}+Ri_a&=(-U_a+m_a\frac{V_{dc}}{2})\\
L\frac{di_b}{dt}+Ri_b&=(-U_b+m_b\frac{V_{dc}}{2})\\
L\frac{di_c}{dt}+Ri_c&=(-U_c+m_c\frac{V_{dc}}{2})
\end{aligned} \quad (19)$$

These equations can be aggregated as a block diagram as illustrated by Fig. 5.

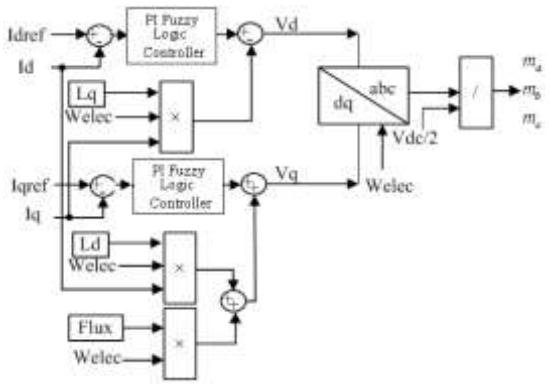

Fig. 5. Control Block diagram of VSC

2.4. Fuzzy Logic PI Controller

The amount of wind energy that can be supplied to the grid and maintain the frequency stability is determined by wind energy control block. The decrease in system frequency would require increased supply of real power from wind generator. The amount of energy support from wind generators is difficult to determine under variable wind speed situations. As the relationship between the real power adjustment in wind generator and input variables are highly nonlinear, the fuzzy-logic based controller is proposed in this paper can help to control the system appropriately. The Fuzzy rules of fuzzy reasoning are mentioned in Table 2 and the membership function of the PI controller is illustrated in Fig. 6.

$$Error = I_{q,d_{ref}} - I_{q,d_{meas}} \tag{20}$$

Table.2.
Fuzzy Rules and Fuzzy Reasoning

Error	***NB***	***N***	***Z***	***P***	***PB***
NB	NB	NB	NB	N	Z
N	NB	NB	N	Z	P
Z	NB	N	Z	P	PB
P	N	Z	P	PB	PB
PB	Z	P	PB	PB	PB

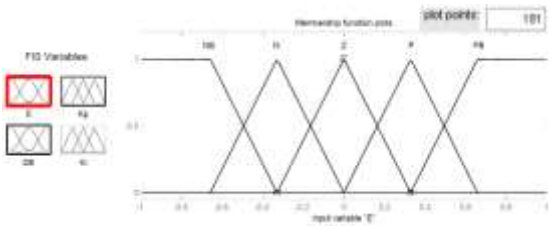

Fig. 6. Membership function of the PI Controller

3. Proposed Control Method of the Wind Farm

In this section, it is assumed to propose the control system to involve the wind farm in controlling the frequency of the power system. For this purpose, it is considered a four-area power system in which the wind farm is located in the first area and is connected to the other areas by transmission lines. The configuration of the four-area system is illustrated in Fig. 6. The wind farm is consisting of N wind turbines, each of them is connected to a VSC, and is finally connected to the power grid through a HVDC line. According to the Fig. 5, to control the output power of the wind farm, the Iq_{ref} signal must be generated properly, as shown in Fig. 7 this is generated from the ΔP_{ref} command and provides the necessary active power changes produced by the wind farm. As illustrated in Fig. 7, the ΔP_{ref} signal is applied to the wind farm to the control system by the frequency deviation of the power system in first area, where the wind farm is located to finally control the wind farm power and participate in the frequency control of the power grid. In Fig. 5, the Iq_{ref} can be achieved by (22), as below. In this system, it is assumed that all of the wind turbines generate the same power. Where P_{G_1} is the active power set point, generated in Fig. 7.

$$i_{qref} = -\frac{1}{N_{Gear}} \frac{P_{G1}}{\frac{3}{2} PN\lambda\omega_m} \tag{21}$$

$$\Delta P_{ref} = P_{ref0} - P_{G1} \tag{22}$$

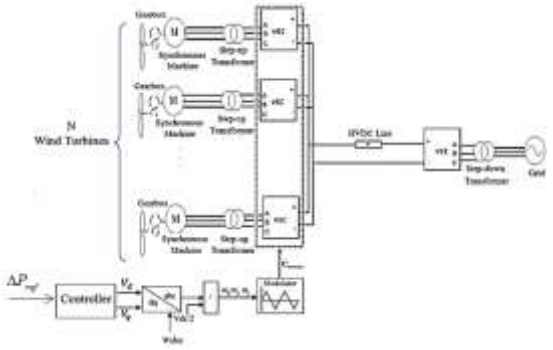

Fig. 7. Wind turbines connection to the power grid to participate in frequency control

4. Simulation Results

A four-area power system connected by five tie lines illustrated in Fig. 8 is taken as a test system in the study. Each area decides steam turbine contains a governor and a generator.

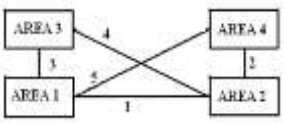

Fig. 8. Four interconnected control area (five tie lines)

The model of the control block diagram of this system is illustrated in Fig. 9.

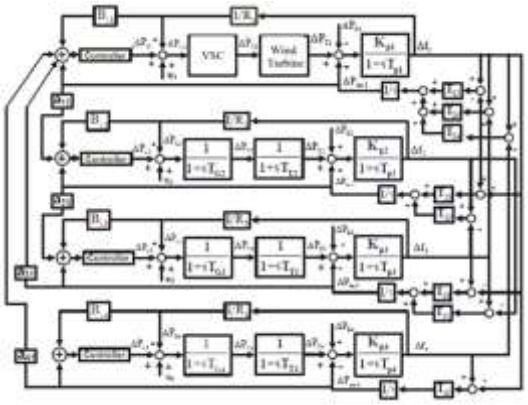

Fig. 9. Four interconnected control area block diagram system

In this system, three different load demand variations as a step load increasing in demand power is applied at t= 3 sec in area 1 and the following figures, represents comparison between two cases, the LFC system without wind farm and with 25% wind farm penetration. The mentioned wind farm system is installed in area 1. However, the wind speed is not constant in the simulation process and is included as a variable parameter by the time as illustrated in Fig. 10.

The Fig. 11 to Fig. 14, illustrate the frequency deviation of the 1st to 4th area, respectively in case of presence and absence of the wind farm while the $\Delta P_D = +0.25 p.u$.

The Figs. 15, 16 and 17, illustrate the active power transmitted from 1st to 2nd, 3rd and 4th area respectively. The case is studied in presence and absence of the wind farm while the $\Delta P_D = +0.25 p.u$.

The Fig. 18 to Fig. 21, illustrate the frequency deviation of the 1st to 4th area, respectively in case of presence and absence of the wind farm while the $\Delta P_D = +0.5 p.u$ and The Figs. 22, 23 and 24, illustrate the active power transmitted from 1st to 2nd, 3rd and 4th area respectively. The case is studied in presence and absence of the wind farm while the $\Delta P_D = +0.5 p.u$.

Fig. 25 to Fig. 28, illustrate the frequency deviation of the 1st to 4th area, respectively in case of presence and absence of the wind farm while the $\Delta P_D = +0.75 p.u$.The Figs. 29, 30 and 31, illustrate the active power transmitted from 1st to 2nd, 3rd and 4th area respectively. The case is studied in presence and absence of the wind farm while the $\Delta P_D = +0.75 p.u$

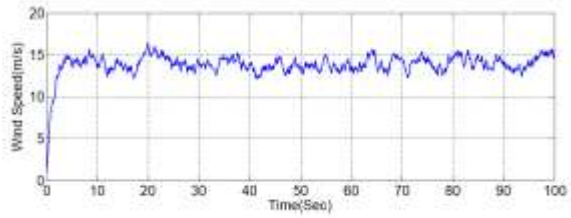

Fig. 10. Wind speed variation due to time

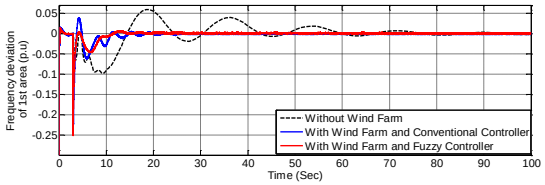

Fig. 11. Frequency deviation of the 1st area

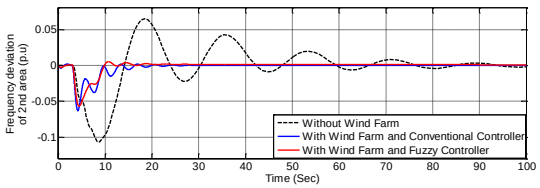

Fig. 12. Frequency deviation of the 2nd area

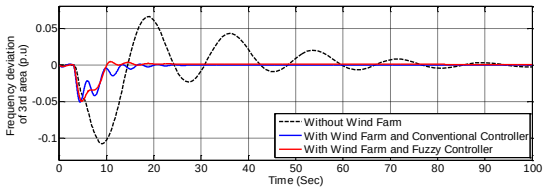

Fig. 13. Frequency deviation of the 3rd area

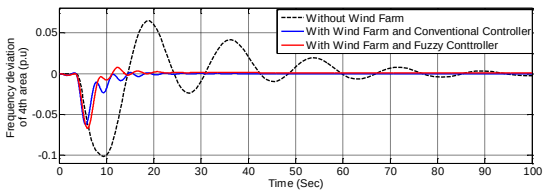

Fig. 14. Frequency deviation of the 4th area

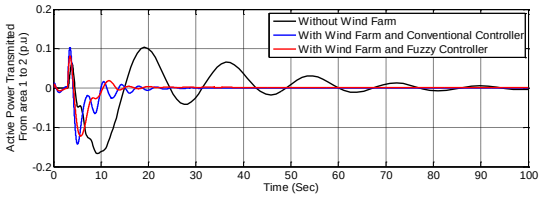

Fig. 15. Active power transmitted from area 1 to 2

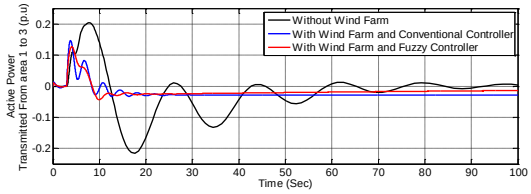

Fig. 16. Active power transmitted from area 1 to 3

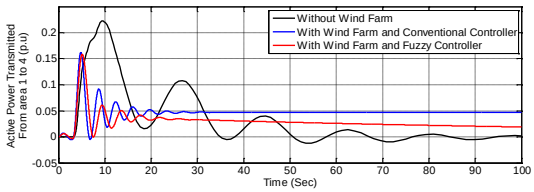

Fig. 17. Active power transmitted from area 1 to 4.

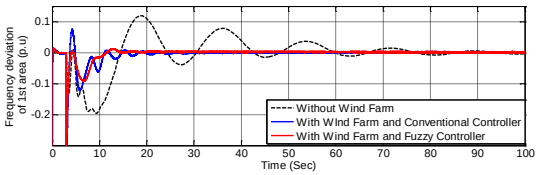

Fig. 18. Frequency deviation of the first area

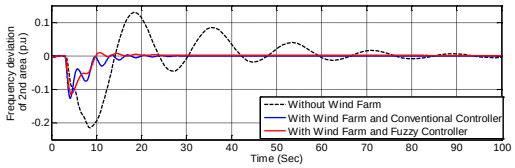

Fig. 19. Frequency deviation of the 2nd area)

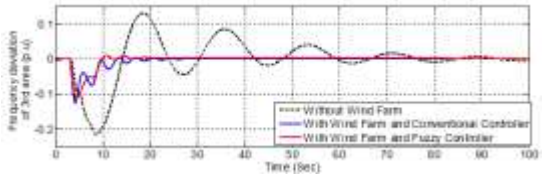

Fig. 20. Frequency deviation of the 3rd area

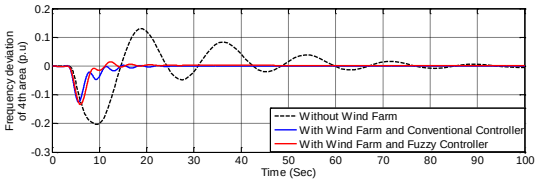

Fig. 21. Frequency deviation of the 4th area

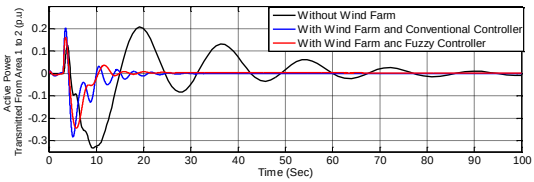

Fig. 22. Active power transmitted from area 1 to 2

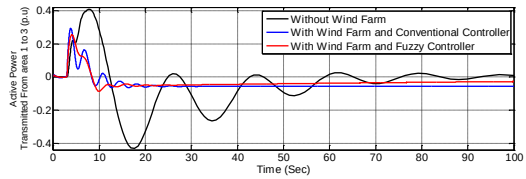

Fig. 23. Active power transmitted from area 1 to 3.

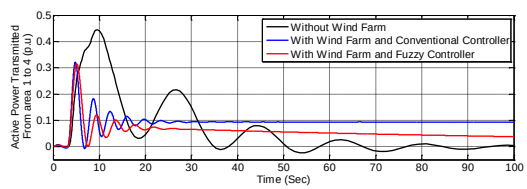

Fig. 24. Active power transmitted from area 1 to 4

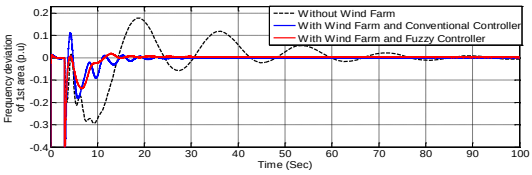

Fig. 25. Frequency deviation of the 1st area

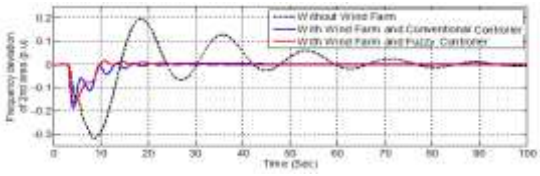

Fig. 26. Frequency deviation of the 2nd area

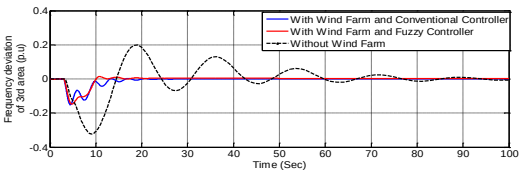

Fig. 27. Frequency deviation of the 3rd area

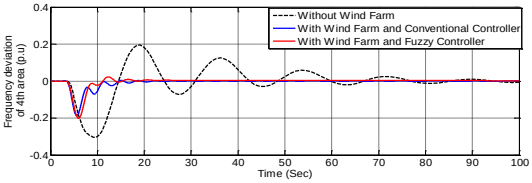

Fig. 28. Frequency deviation of the 4th area

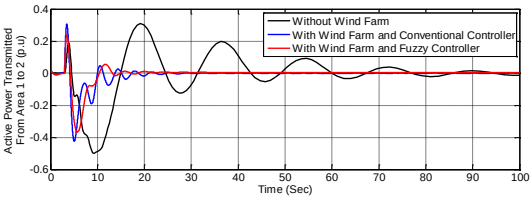

Fig. 29. Active power transmitted from area 1 to 2

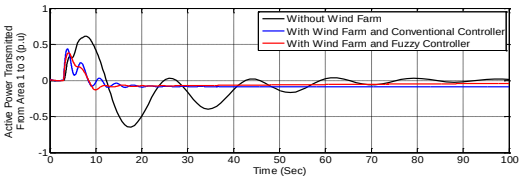

Fig. 30. Active power transmitted from area 1 to 3

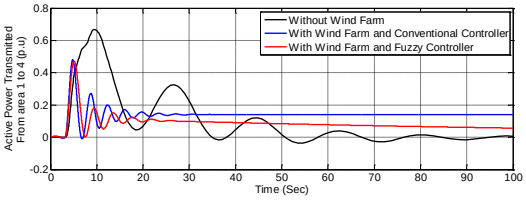

Fig. 31. Active power transmitted from area 1 to 4

It can be seen from the previous diagrams that the sudden increase in load demand causes the grid frequency to drop suddenly. This is caused by the sudden increase in load demand and the inability of the generators of the power system to provide enough active power rapidly. However, it can be inferred that while the wind farm is not cooperated in the task of frequency controlling of the grid, the frequency dynamics and compensation are much slower than while the wind farm system is in operation with the proposed method and control system. Finally, in Table 3, it is assumed to compare the parameter of settling time of damping frequency fluctuations in the power system during sudden load changes. For more investigation, three cases of absence of wind farm (power system with traditional frequency control method) and presence of wind farm (proposed frequency control method, with and without Fuzzy logic controller) are considered. In this comparison, it is inferred that the proposed method was able to significantly improve the parameter of settling time in damping frequency fluctuations during rapid load changes, which indicates the appropriate effectiveness of the proposed system.

Table.3.
Comparison between the presence and absence of the wind farm in settling time parameter of frequency deviation response

	1st Area Settling Time (Sec)		***2nd Area Settling Time (Sec)***		***3rd Area Settling Time (Sec)***		***4th Area Settling Time (Sec)***	
Case 1: Without Wind Farm	$\Delta P_D = +0.25p.u\Delta P_D = +0.50p.u\Delta P_D = +0.75p.u$	87.51	$\Delta P_D = +0.25p.u\Delta P_D = +0.50p.u\Delta P_D = +0.75p.u$	87.51	$\Delta P_D = +0.25p.u\Delta P_D = +0.50p.u\Delta P_D = +0.75p.u$	87.51	$\Delta P_D = +0.25p.u\Delta P_D = +0.50p.u\Delta P_D = +0.75p.u$	87.51
Case 2: Wind Farm & Conventional Controller	$\Delta P_D = +0.25p.u\Delta P_D = +0.50p.u\Delta P_D = +0.75p.u$	7.6	$\Delta P_D = +0.25p.u\Delta P_D = +0.50p.u\Delta P_D = +0.75p.u$	12.9	$\Delta P_D = +0.25p.u\Delta P_D = +0.50p.u\Delta P_D = +0.75p.u$	13.1	$\Delta P_D = +0.25p.u\Delta P_D = +0.50p.u\Delta P_D = +0.75p.u$	14.2
Case 3: Wind Farm & Fuzzy Controller	$\Delta P_D = +0.25p.u\Delta P_D = +0.50p.u\Delta P_D = +0.75p.u$	5.7	$\Delta P_D = +0.25p.u\Delta P_D = +0.50p.u\Delta P_D = +0.75p.u$	12.2	$\Delta P_D = +0.25p.u\Delta P_D = +0.50p.u\Delta P_D = +0.75p.u$	12.4	$\Delta P_D = +0.25p.u\Delta P_D = +0.50p.u\Delta P_D = +0.75p.u$	10.45
Settling Time Improvement (%)	From Case 1 to 2	91.3%	From Case 1 to 2	85.2%	From Case 1 to 2	85%	From Case 1 to 2	83.77%
	From Case 1 to 3	93.4%	From Case 1 to 3	86%	From Case 1 to 3	85.8%	From Case 1 to 3	88%
	From Case 2 to 3	25%	From Case 2 to 3	5.4%	From Case 2 to 3	5.3%	From Case 2 to 3	26.4%

5. Conclusion

In this paper, a new control method based on fuzzy logic controller is applied to the wind farm system connected to the grid via HVDC link to cooperate in frequency control of the power system. The main advantage of the proposed control system is the accurate controllability of the wind farm in frequency control of the grid with fast response even during wind speed variations. To verify the appropriate performance of the proposed method, the wind farm system is simulated on a four-area interconnected grid in three different scenarios. First, not the presence of a wind farm (using traditional power system). Second, in the presence of the wind farm with traditional PI controller and finally, in the presence of the wind farm with the proposed fuzzy logic controller. The load demand varies for a sudden increase of 0. 25p.u, 0.5p.u and 0.75p.u on the 1st area. The results of three scenarios were compared to each other accurately. It is inferred that the dynamic response of the wind farm system to compensate for the frequency fluctuations was significantly faster than two other scenarios.

References

[1]. H. Wang et al., "Model Predictive Control of PMSG-Based Wind Turbines for Frequency Regulation in an Isolated Grid," in IEEE Transactions on Industry Applications, vol. 54, no. 4, pp. 3077-3089, July-Aug. 2018, doi: 10.1109/TIA.2018.2817619.

[2]. Francisco, Díaz-González, “Coordinated operation of wind turbines and flywheel storage for primary frequency control support”, Electrical Power and Energy System, vol 68 .pp. 313-326. 2015, doi: 10.1016/j.ijepes.2014.12.062.

[3]. K. Sun et al., "Frequency Compensation Control Strategy of Energy Storage in the Wind-energy storage Hybrid System for Improving Frequency Response Performance," 2019 IEEE Industry Applications Society Annual Meeting, 2019, pp. 1-8, doi: 10.1109/IAS.2019.8912404.

[4]. Z. Wang et al., "Research on the active power coordination control system for wind/photovoltaic/energy storage," 2017 IEEE Conference on Energy Internet and Energy System Integration (EI2), 2017, pp. 1-5, doi: 10.1109/EI2.2017.8245403.

[5]. L. Miao, J. Wen, H. Xie, C. Yue and W. Lee, "Coordinated Control Strategy of Wind Turbine Generator and Energy Storage Equipment for Frequency Support," in IEEE Transactions on Industry Applications, vol. 51, no. 4, pp. 2732-2742, July-Aug. 2015, doi: 10.1109/TIA.2015.2394435.

[6]. A. Abedini and A. Nasiri, "Applications of super capacitors for PMSG wind turbine power smoothing," 2008 34th Annual Conference of IEEE Industrial Electronics, 2008, pp. 3347-3351, doi: 10.1109/IECON.2008.4758497.

[7]. Yujun Li, Zeren Zhang, Yong Yang, Yingyi Li, Hairong Chen, Zheng Xu, Coordinated control of wind farm and VSC–HVDC system using capacitor energy and kinetic energy to improve inertia level of power systems, International Journal of Electrical Power & Energy Systems, Volume 59, 2014, Pages 79-92, ISSN 0142-0615, doi: 10.1016/j.ijepes.2014.02.003.

[8]. Y. Ma, G. Zou, M. Hou, Q. Dong and J. Yang, "Optimal dispatching for active distribution network with wind-battery hybrid power system," 2017 IEEE Electrical Power and Energy Conference (EPEC), 2017, pp. 1-6, doi: 10.1109/EPEC.2017.8286160.

[9]. S. Tobaru, F. Conteh, T. Senjyu, A. M. Howlader and T. Funabashi, "Optimal sizing of PV-wind-battery power system considering demand response programs," 2017 IEEE 12th International Conference on Power Electronics and Drive Systems (PEDS), 2017, pp. 162-165, doi: 10.1109/PEDS.2017.8289232.

[10]. A. R. Boynuegri and Y. Eren, "An Approach to Design Power Management Structure for Hybrid Power Systems: A case study on Wind- Battery-Ultracapacitor Hybrid Power System," 2018 International Conference on Smart Energy Systems and Technologies (SEST), 2018, pp. 1-6, doi: 10.1109/SEST.2018.8495660.

[11]. D. Mende, T. Hennig, A. Akbulut, H. Becker and L. Hofmann, "Dynamic frequency support with DFIG wind turbines-A system study," 2016 IEEE Electrical Power and Energy Conference (EPEC), 2016, pp. 1-7, doi: 10.1109/EPEC.2016.7771694.

[12]. N. Elmouhi, A. Essadki, H. Elaimani and R. Chakib, "Evaluation of the Inertial Response of Variable Speed Wind Turbines Based on DFIG using Backstepping for a Frequency Control," 2019 International Conference on Wireless Technologies, Embedded and Intelligent Systems (WITS), 2019, pp. 1-6, doi: 10.1109/WITS.2019.8723766.

[13]. O. Awedni, A. Masmoudi and L. Krichen, "Power Control of DFIG-Based Wind Farm for System Frequency Support," 2018 15th International Multi-Conference on Systems, Signals & Devices (SSD), 2018, pp. 1298-1304, doi: 10.1109/SSD.2018.8570400.

[14]. P. Sonkar and O. P. Rahi, "Investigation on DFIG based wind turbine for short term frequency regulation techniques," 2017 4th International Conference on Power, Control & Embedded Systems (ICPCES), 2017, pp. 1-6, doi: 10.1109/ICPCES.2017.8117659.

[15]. X. Hua, X. Hongyuan and L. Na, "Control strategy of DFIG wind turbine in primary frequency regulation," 2018 13th IEEE Conference on Industrial Electronics and Applications (ICIEA), 2018, pp. 1751-1755, doi: 10.1109/ICIEA.2018.8397992.

[16]. D. Li, M. Cai, W. Yang and J. Wang, "Study of Doubly Fed Induction Generator Wind Turbines for Primary Frequency Control," 2020 IEEE 4th Conference on Energy Internet and Energy System Integration (EI2), 2020, pp. 2690-2695, doi: 10.1109/EI250167.2020.9346644.

[17]. T. van Engelen, E. van der Hooft, and P. Schaak, “Development of wind turbine control algorithms for industrial use,” In European Wind Energy Conference Copenhagen, Denmark , pp. 1098 – 1101, 2001.

[18]. Y. Wu, W. Yang, Y. Hu and D. P. Quoc, "Frequency regulation at a wind farm using time-varying inertia and droop controls," 2018 IEEE/IAS 54th Industrial and Commercial Power Systems Technical Conference (I&CPS), 2018, pp. 1-9, doi: 10.1109/ICPS.2018.8369978.

[19]. P. Dubucq and G. Ackermann, "Frequency control in coupled energy systems with high penetration of renewable energies," 2015 International Conference on Clean Electrical Power (ICCEP), 2015, pp. 326-332, doi: 10.1109/ICCEP.2015.7177643.

[20]. A. Junyent-Ferr, Y. Pipelzadeh and T. C. Green, "Blending HVDC-Link Energy Storage and Offshore Wind Turbine Inertia for Fast Frequency Response," in IEEE Transactions on Sustainable Energy, vol. 6, no. 3, pp. 1059-1066, July 2015, doi: 10.1109/TSTE.2014.2360147.

[21]. Ju Liu, Wei Yao, Jinyu Wen and Yao Long, "Short-term frequency support of power system from wind farms using energy storage system," 2015 IEEE Power & Energy Society General Meeting, 2015, pp. 1-5, doi: 10.1109/PESGM.2015.7286182.

[22]. G. Xu, L. Xu and J. Morrow, "System frequency support using wind turbine kinetic energy and energy storage system," 2nd IET Renewable Power Generation Conference (RPG 2013), 2013, pp. 1-4, doi: 10.1049/cp.2013.1812.

[23]. D. Mende, T. Hennig, A. Akbulut, H. Becker and L. Hofmann, "Dynamic frequency support with DFIG wind turbines - A system study," 2016 IEEE Electrical Power and Energy Conference (EPEC), 2016, pp. 1-7, doi: 10.1109/EPEC.2016.7771694.

[24]. Kazemi Golkhandan, Reza; Torkaman, Hossein; Aghaebrahimi, Mohammad Reza; Keyhani, Ali: 'Load frequency control of smart isolated power grids with high wind farm penetrations', IET Renewable Power Generation, 2020, 14, (7), p. 1228-1238, doi: 10.1049/iet-rpg.2019.0601.

[25]. Simões, M.G.; Bubshait, A. Frequency Support of Smart Grid Using Fuzzy Logic-Based Controller for Wind Energy Systems. Energies 2019, 12, 1550, doi:10.3390/en12081550.

[26]. J. He, K. Wu, L. Huang, H. Xin, C. Lu and H. Wang, "A Coordinated Control Scheme to Realize Frequency Support of PMSG-Based Wind Turbines in Weak Grids," 2018 IEEE Power & Energy Society General Meeting (PESGM), 2018, pp. 1-5, doi: 10.1109/PESGM.2018.8586541.

[27]. T. Sato, F. Asharif, A. Umemura, R. Takahashi and J. Tamura, "Cooperative Virtual Inertia and Reactive Power Control of PMSG Wind Generator and Battery for Improving Transient Stability of Power System," 2020 IEEE International Conference on Power and Energy (PECon), 2020, pp. 101-106, doi: 10.1109/PECon48942.2020.9314621.

[28]. Y. Wu, W. Yang, Y. Hu and D. P. Quoc, "Frequency regulation at a wind farm using time-varying inertia and droop controls," 2018 IEEE/IAS 54th Industrial and Commercial Power Systems Technical Conference (I&CPS), 2018, pp. 1-9, doi: 10.1109/ICPS.2018.8369978.

[29]. P. Mahish and A. K. Pradhan, "Distributed Synchronized Control in Grid Integrated Wind Farms to Improve Primary Frequency Regulation," in IEEE Transactions on Power Systems, vol. 35, no. 1, pp. 362-373, Jan. 2020, doi: 10.1109/TPWRS.2019.2928394.

[30]. A. Bidadfar, O. Saborío-Romano, N. A. Cutululis and P. E. Sørensen, "Control of Offshore Wind Turbines Connected to Diode-Rectifier-Based HVdc Systems," in IEEE Transactions on Sustainable Energy, vol. 12, no. 1, pp. 514-523, Jan. 2021, doi: 10.1109/TSTE.2020.3008606.

[31]. M. M. Kabsha and Z. H. Rather, "A New Control Scheme for Fast Frequency Support From HVDC Connected Offshore Wind Farm in Low-Inertia System," in IEEE Transactions on Sustainable Energy, vol. 11, no. 3, pp. 1829-1837, July 2020, doi: 10.1109/TSTE.2019.2942541.

[32]. Y. Xiong et al., "Two-Level Combined Control Scheme of VSC-MTDC Integrated Offshore Wind Farms for Onshore System Frequency Support," in IEEE Transactions on Power Systems, vol. 36, no. 1, pp. 781-792, Jan. 2021, doi: 10.1109/TPWRS.2020.2998579.

[33]. L. Guo et al., "Double-Layer Feedback Control Method for Synchronized Frequency Regulation of PMSG-Based Wind Farm," in IEEE Transactions on Sustainable Energy, vol. 12, no. 4, pp. 2423-2435, Oct. 2021, doi: 10.1109/TSTE.2021.3096724.

[34]. N. Sa-ngawong and I. Ngamroo, "Optimal fuzzy logic-based adaptive controller equipped with DFIG wind turbine for frequency control in stand alone power system," 2013 IEEE Innovative Smart Grid Technologies-Asia (ISGT Asia), 2013, pp. 1-6, doi: 10.1109/ISGT-Asia.2013.6698773.

[35]. C. -H. Lin and Y. -K. Wu, "Overview of Frequency-Control Technologies for a VSC-HVDC-Integrated Wind Farm," in IEEE Access, vol. 9, pp. 112893-112921, 2021, doi: 10.1109/ACCESS.2021.3102829.

[36]. Hassan Bevrani, Hêmin Golpîra, Arturo Román Messina, Nikos Hatziargyriou, Federico Milano, Toshifumi Ise, Power system frequency control: An updated review of current solutions and new challenges, Electric Power Systems Research, Volume 194, 2021, 10711, doi:10.1016/j.epsr.2021.107114.

[37]. N. G. Khani, M. Abedi, G. B. Gharehpetian and G. H. Riahy, "Offshore Wind Farm Power Control Using HVdc Link," in Canadian Journal of Electrical and Computer Engineering, vol. 39, no. 2, pp. 168-173, Spring 2016, doi: 10.1109/CJECE.2016.2520664.